SUPPLEMENTAL MATERIAL for

Bias-adjusted projections of snow cover over eastern Canada using an ensemble of regional climate models

by Émilie Bresson, Éric Dupuis and Pascal Bourgault

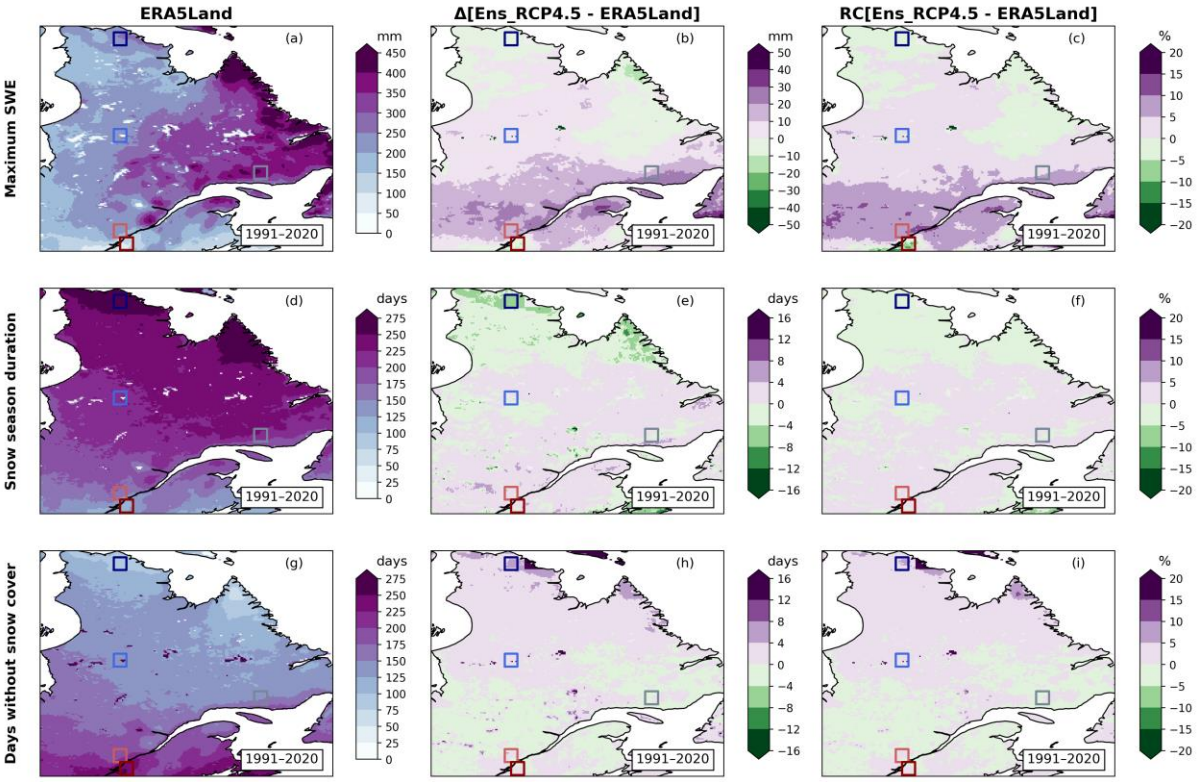

Fig. S1 Annual maximum SWE (first row), snow season duration (second row) and days without snow cover (third row) for ERA5-Land (left), difference (middle) and relative change (right) between the RCP4.5 ensemble and ERA5-Land for the 1991–2020 period

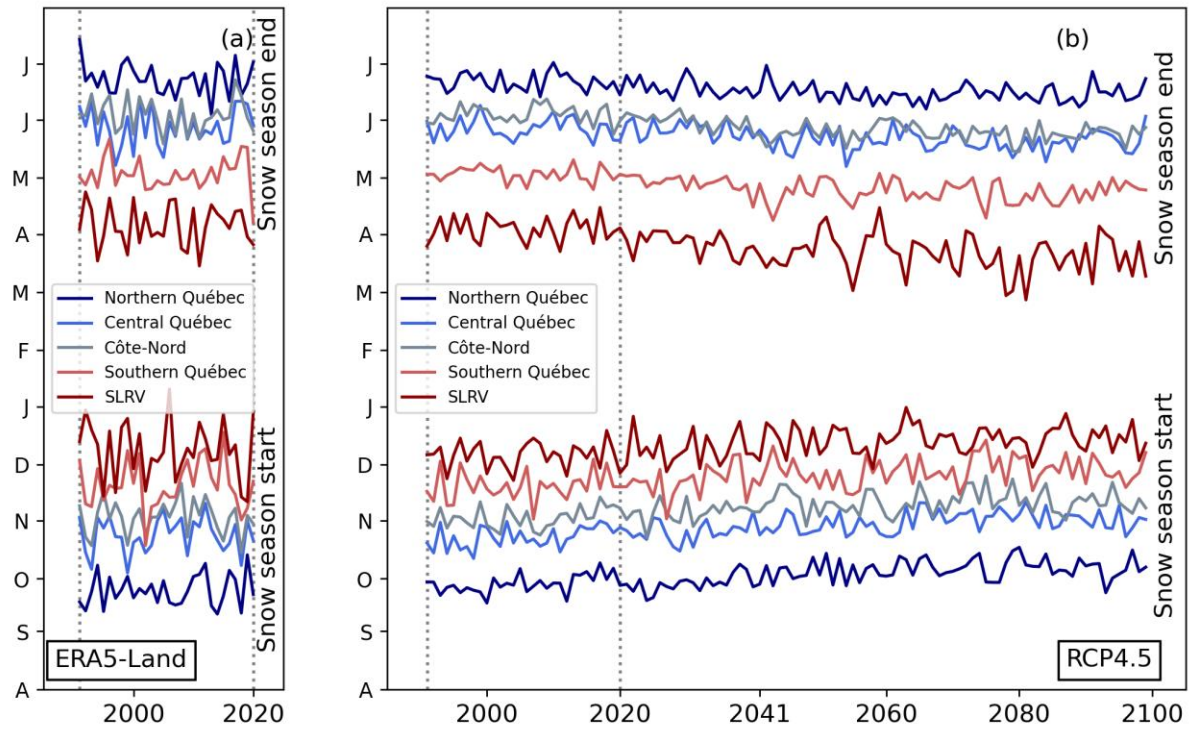

Fig. S2 Time series of snow season start (bottom) and snow season end (top) for ERA5-Land (a) and the RCP4.5 ensemble (b) for the five regions of interest. Dashed gray vertical lines encompass the historical period (1991–2020).

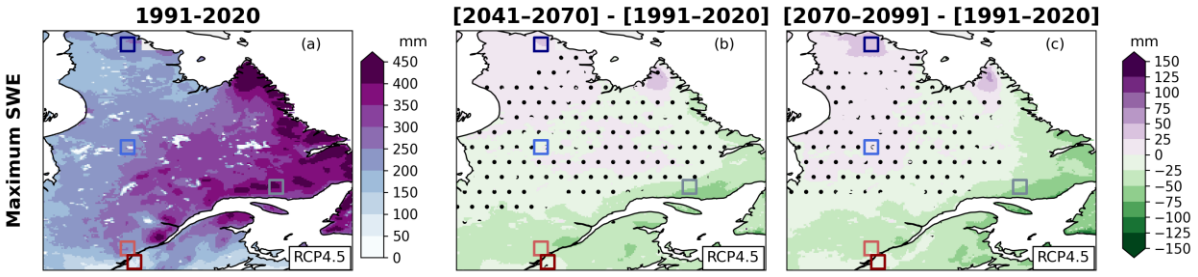

Fig. S3 Annual maximum SWE for 1991–2020 (a), and differences between the 1991–2020 period and 2041–2070 (b) or 2070–2099 (c). Dotted areas are where less than 80 % of the simulations in the ensemble agree on the sign of change. Results are presented for the RCP4.5 ensemble.

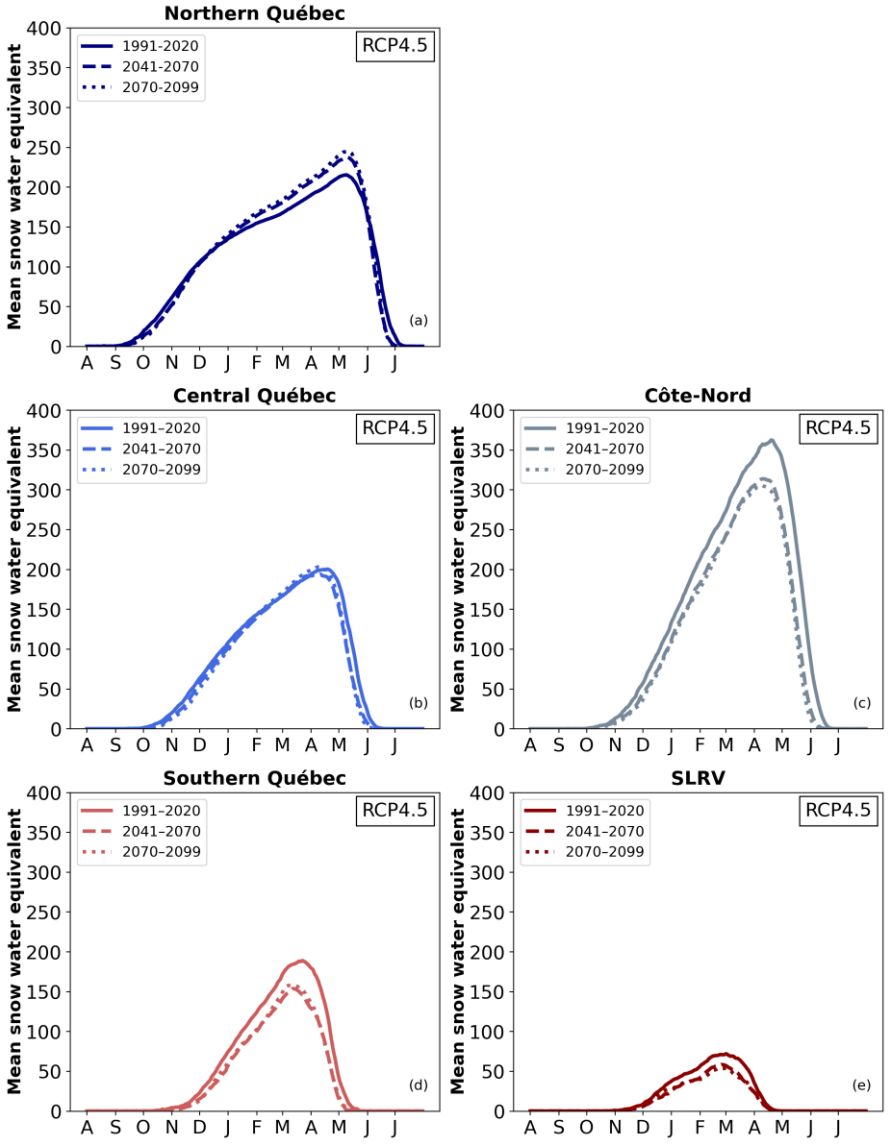

Fig. S4 Annual cycle of SWE for the RCP4.5 ensemble in the five analysis regions.

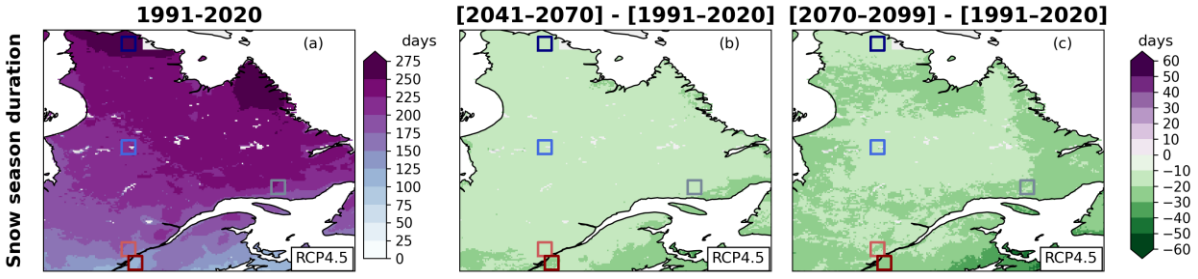

Fig. S5 Annual snow season duration for 1991–2020 (a), and differences between the 1991–2020 period and 2041–2070 (b) or 2070–2099 (c). Dotted areas are where less than 80 % of the simulations in the ensemble agree on the sign of change. Results are presented for the RCP4.5 ensemble.

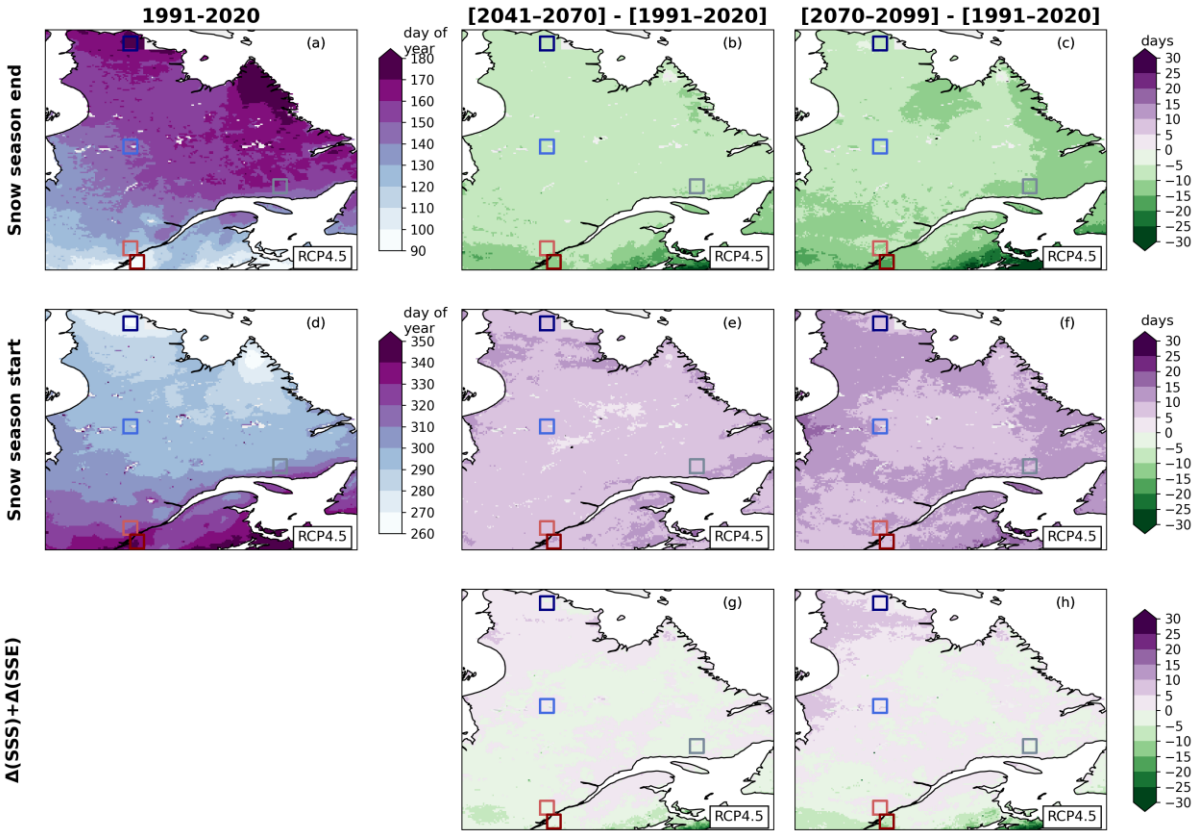

Fig. S6 Snow season end (top), snow season start (middle) and the sum of the change in timing of snow season start and change in timing of snow season end, for 1991–2020 (left), and differences between the historical period (1991–2020) and 2041–2070 (centre) and 2070–2099 (right). Results are presented for the RCP4.5 ensemble.

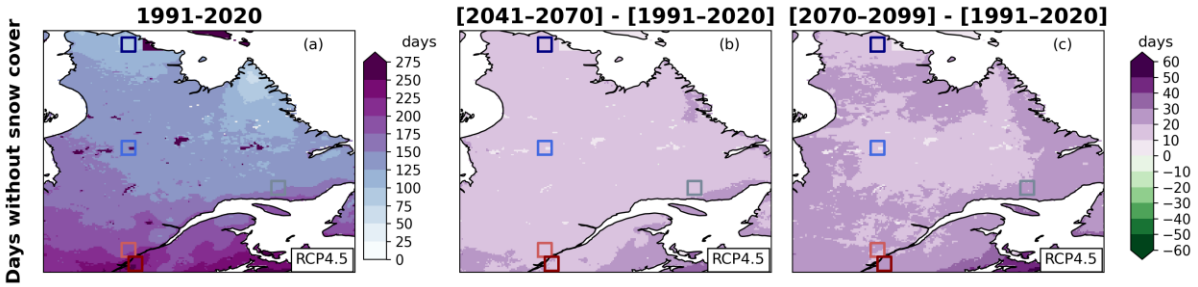

Fig. S7 Annual days without snow cover for 1991–2020 (a), and differences between the 1991–2020 period and 2041–2070 (b) or 2070–2099 (c). Dotted areas are where less than 80 % of the simulations in the ensemble agree on the sign of change. Results are presented for the RCP4.5 ensemble.

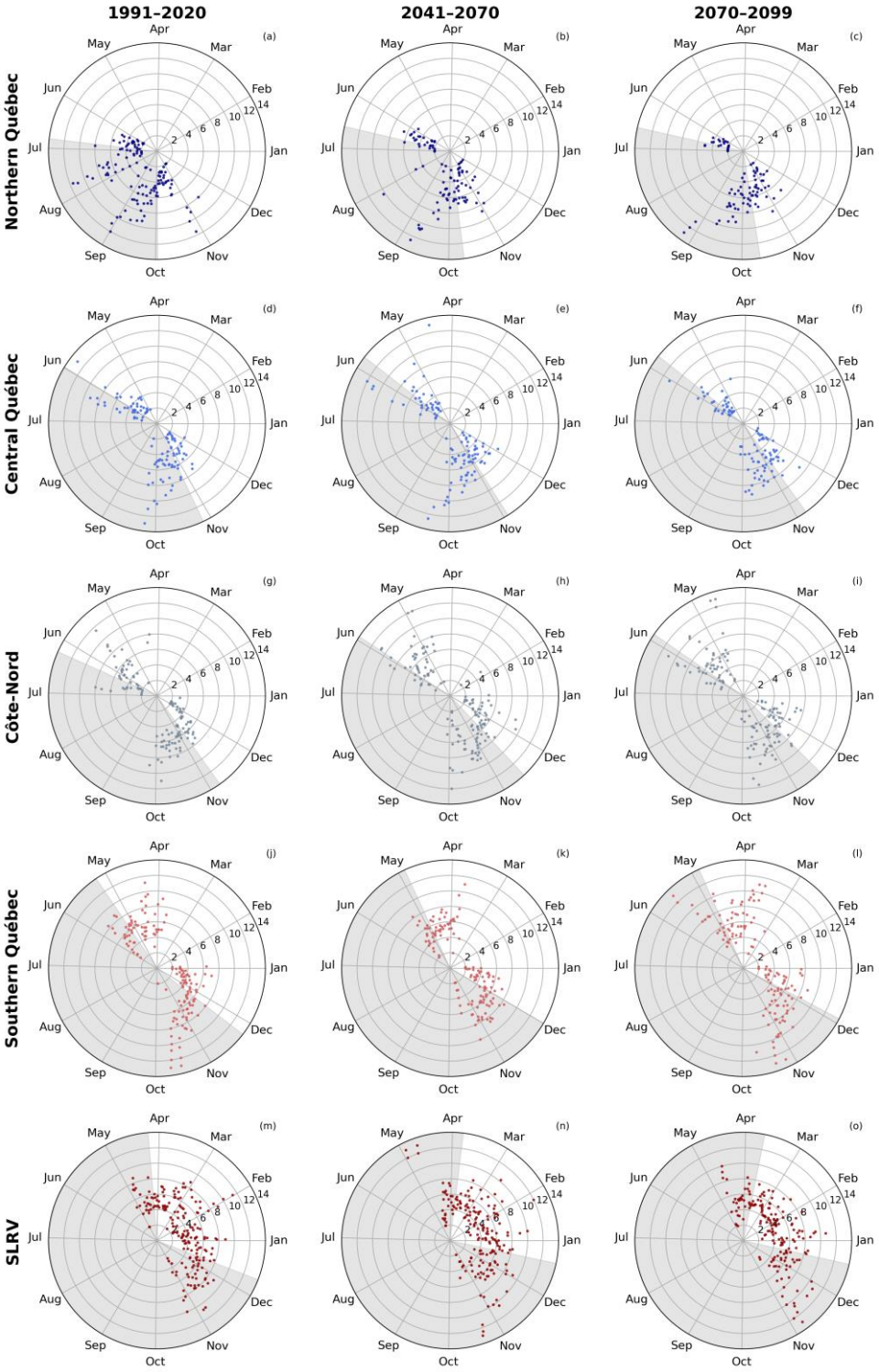

Fig. S8 Length of sequences of 2 to 13 consecutive days without snow cover (radius) as a function of the day of the year (angle) for the RCP4.5 ensemble. The white part of each figure is the mean snow season for the studied period and region. The months are labelled at the first day of the month. Results are presented per region (rows) and for 1991–2020 (left), 2041–2070 (centre) and 2070–2099 (right).

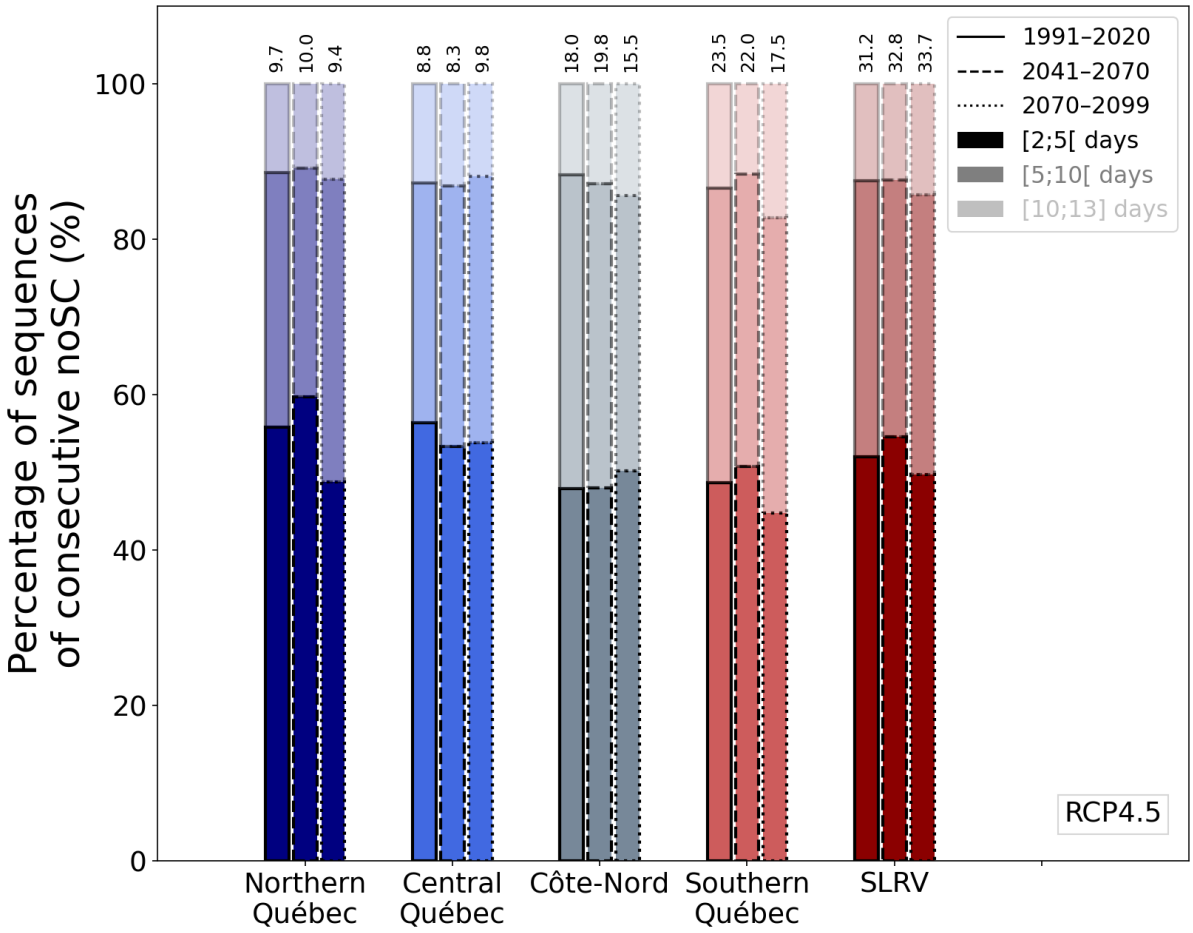

Fig. S9 Percentage of noSCseq during the snow season for the historical period 1991–2020 (lines), 2041-2070 (dashed lines) and 2070–2099 (dotted lines) for the five regions of interest. Three duration ranges are presented with different transparencies: [2;5[, [5;10[and [10;13] consecutive days for the RCP4.5 ensemble. Values on the top of each bar correspond to the total number of noSCseq during the snow season for each region and period.

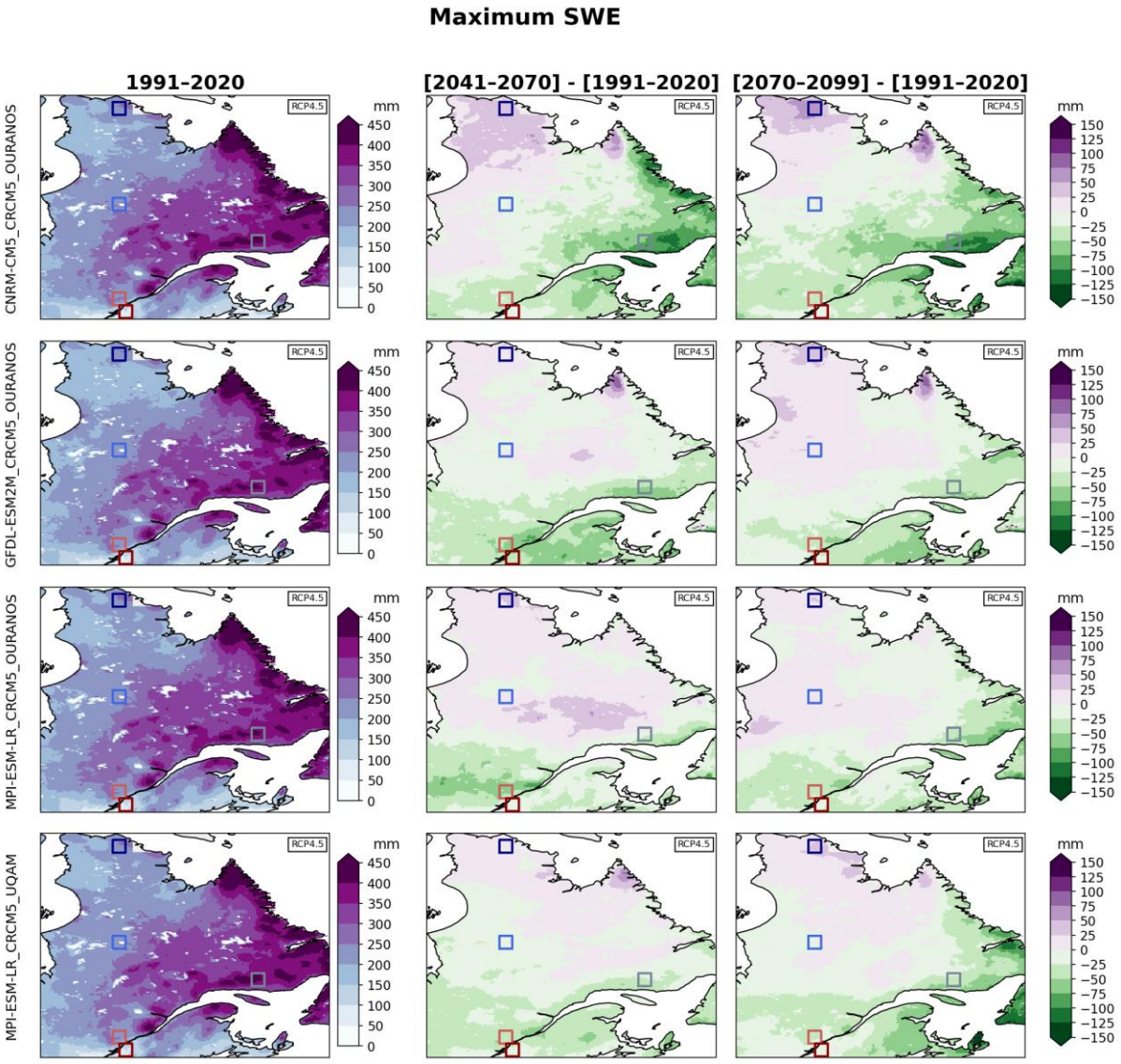

Fig. S10 Annual maximum SWE for 1991–2020 (left column), and differences between the 1991–2020 period and 2041–2070 (centre column) or 2070–2099 (right column). Results are presented for each simulation (row) of the RCP4.5 ensemble.

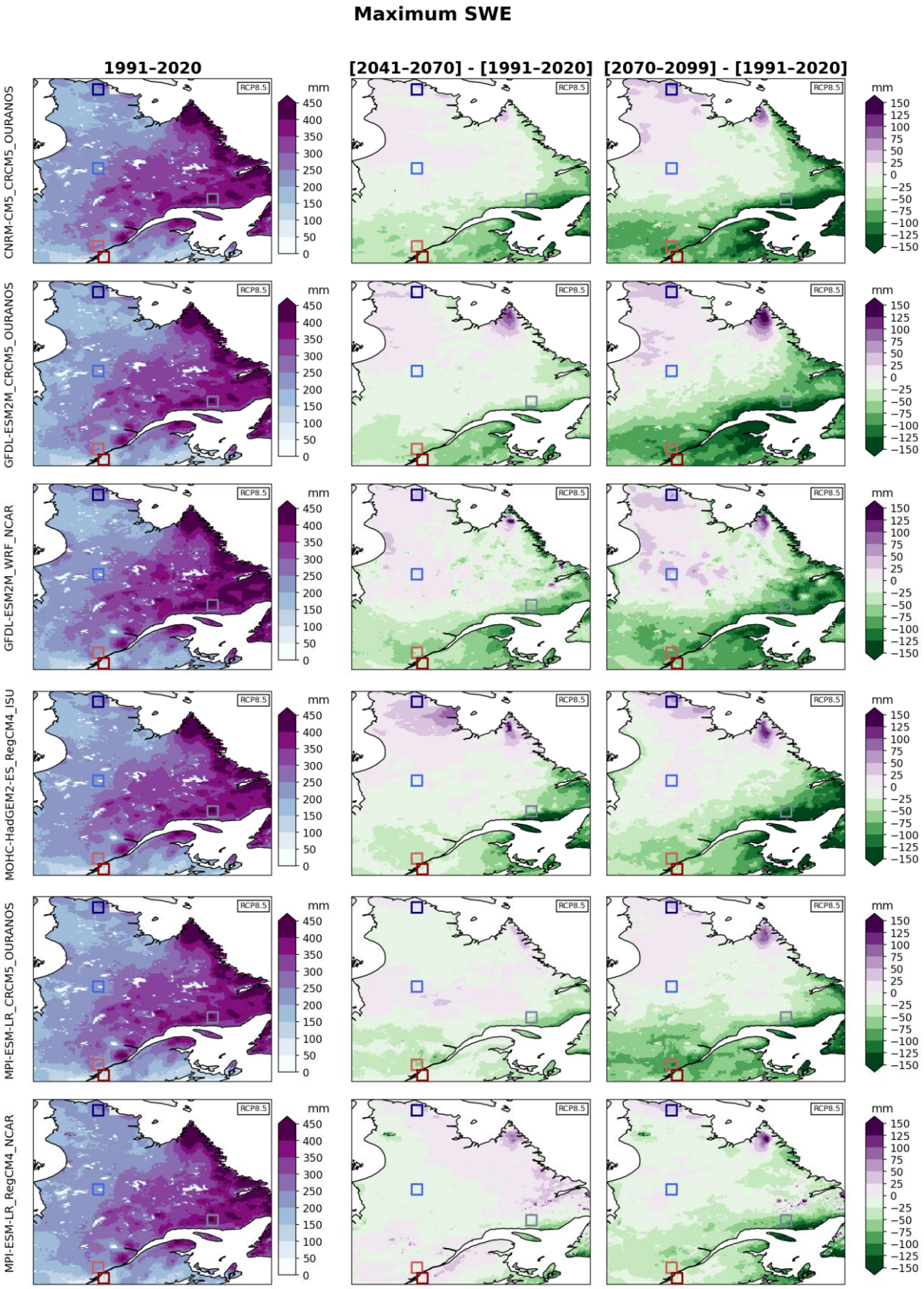

Fig. S11 Annual maximum SWE for 1991–2020 (left column), and differences between the 1991–2020 period and 2041–2070 (centre column) or 2070–2099 (right column). Results are presented for each simulation (row) of the RCP8.5 ensemble.

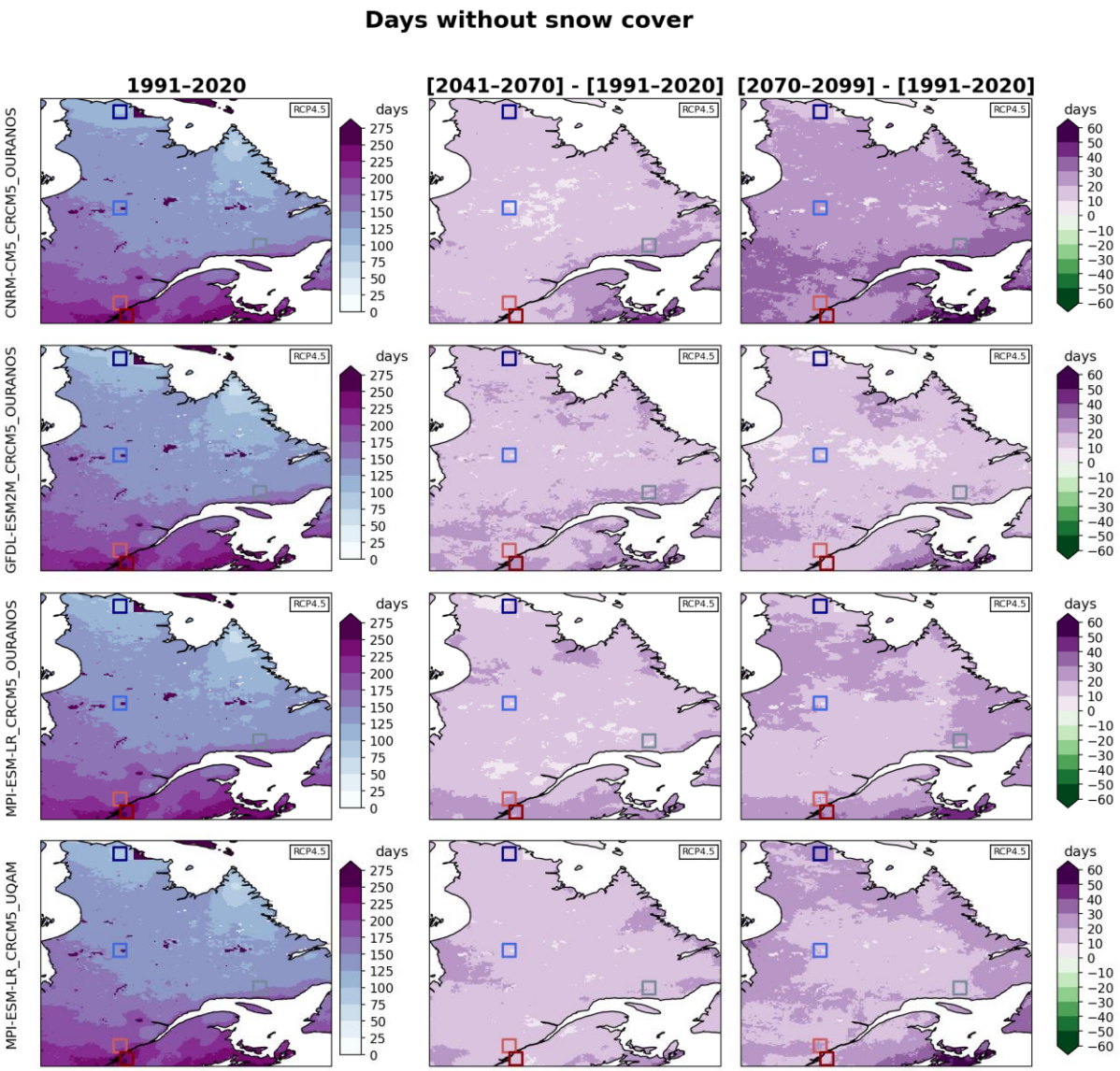

Fig. S12 Annual days without snow cover for 1991–2020 (left column), and differences between the 1991–2020 period and 2041–2070 (centre column) or 2070–2099 (right column). Results are presented for each simulation (row) of the RCP4.5 ensemble.

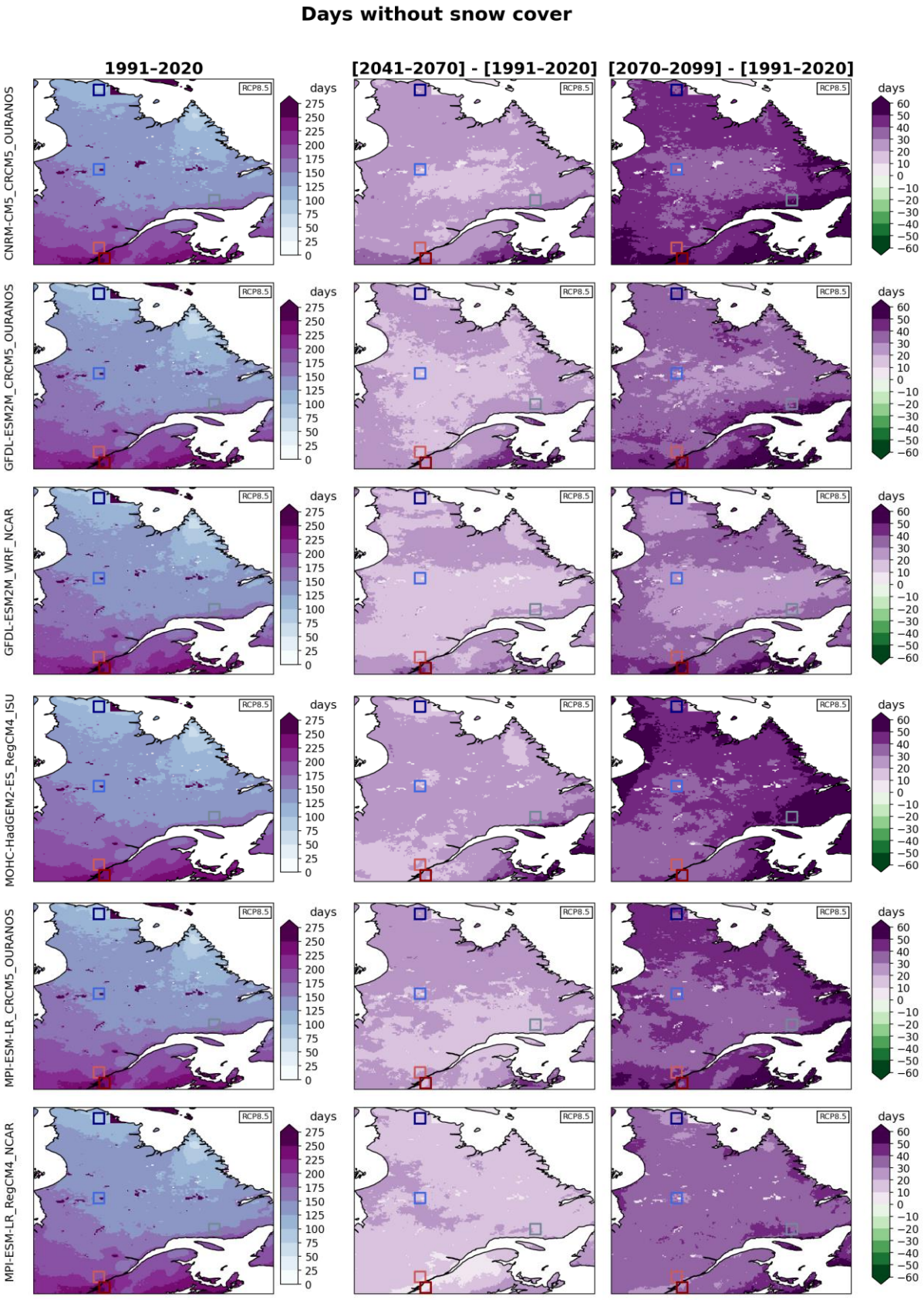

Fig. S13 Annual days without snow cover for 1991–2020 (left column), and differences between the 1991–2020 period and 2041–2070 (centre column) or 2070–2099 (right column). Results are presented for each simulation (row) of the RCP8.5 ensemble.

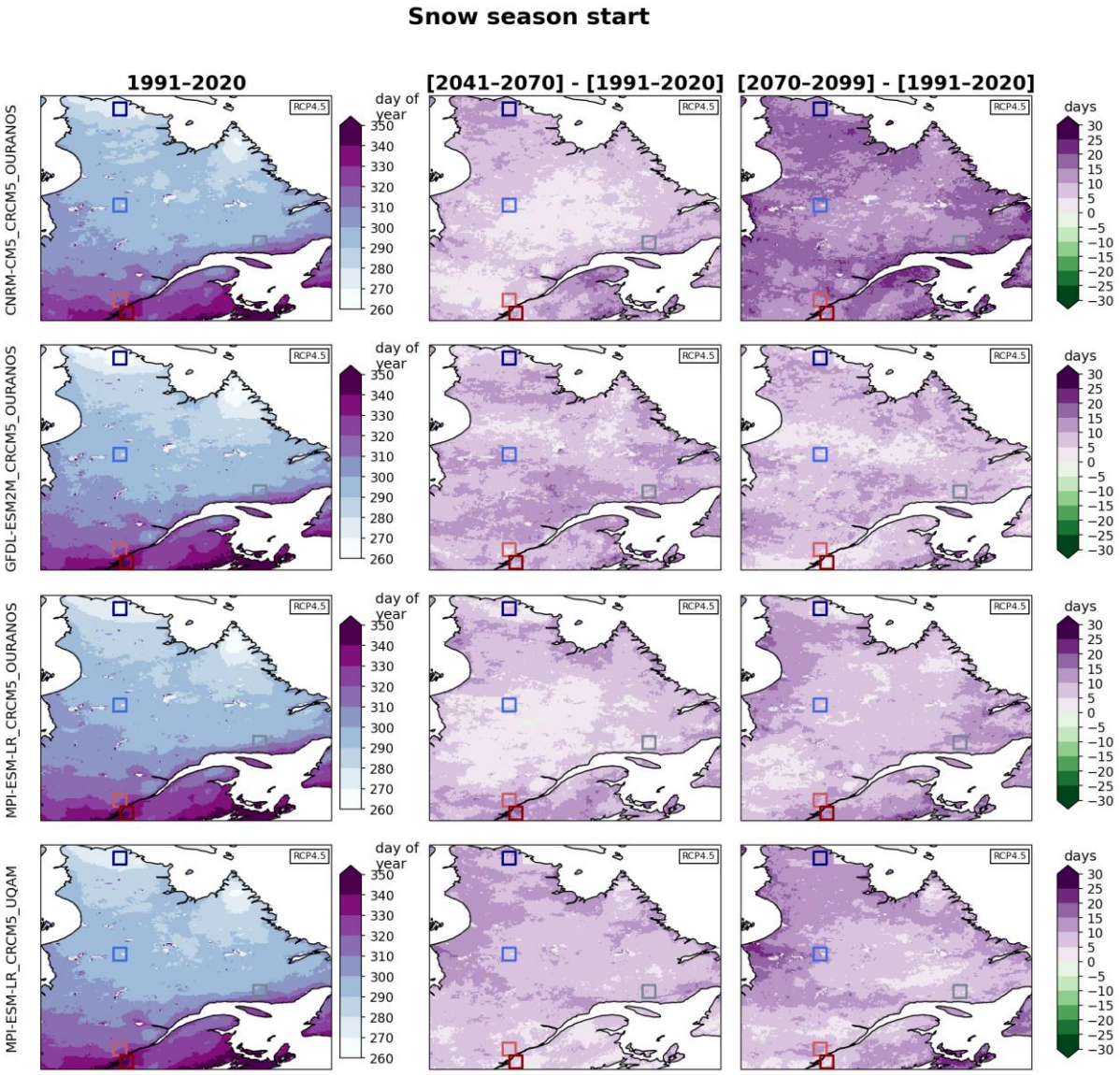

Fig. S14 Annual snow season start for 1991–2020 (left column), and differences between the 1991–2020 period and 2041–2070 (centre column) or 2070–2099 (right column). Results are presented for each simulation (row) of the RCP4.5 ensemble

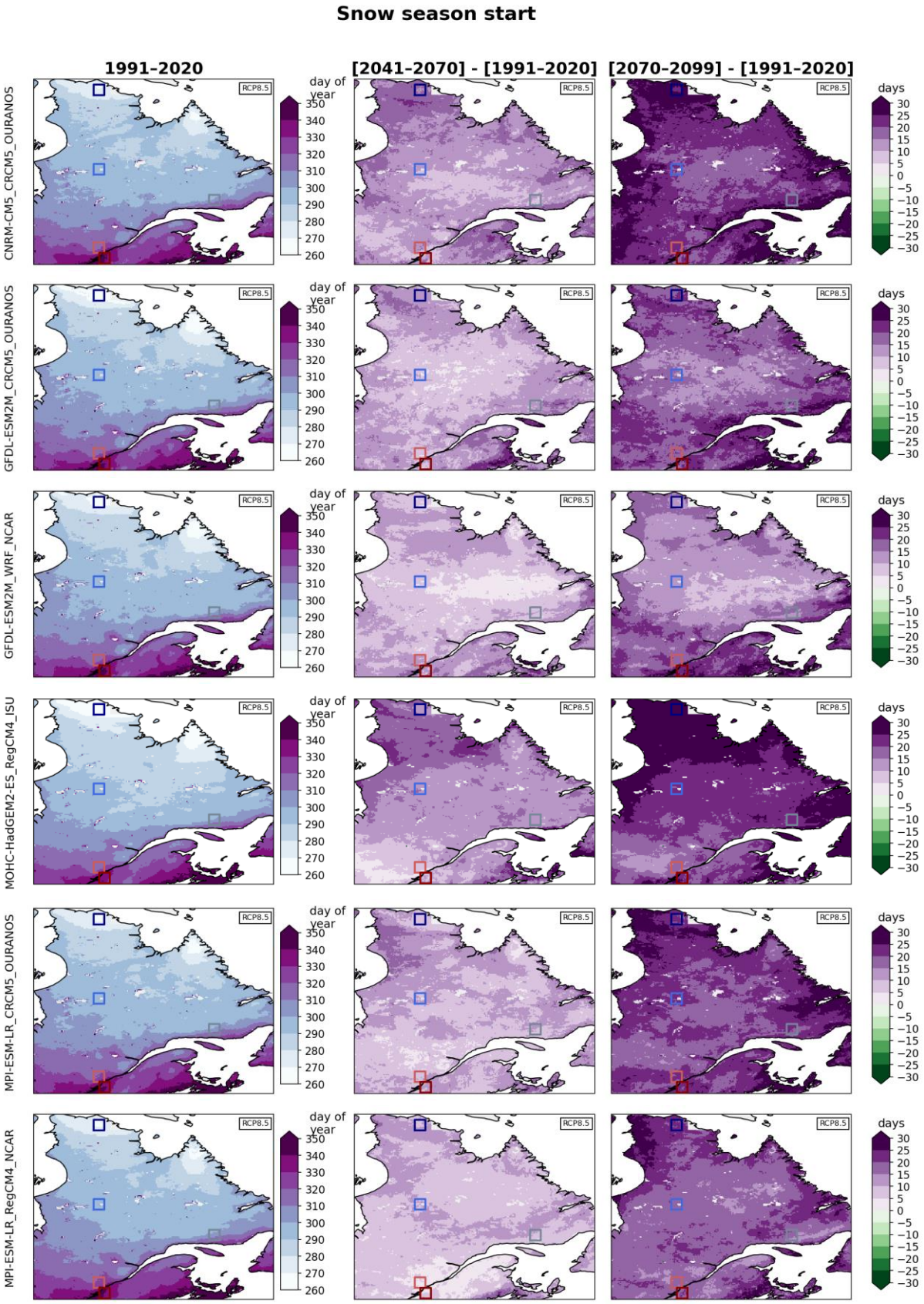

Fig. S15 Annual snow season start for 1991–2020 (left column), and differences between the 1991–2020 period and 2041–2070 (centre column) or 2070–2099 (right column). Results are presented for each simulation (row) of the RCP8.5 ensemble.

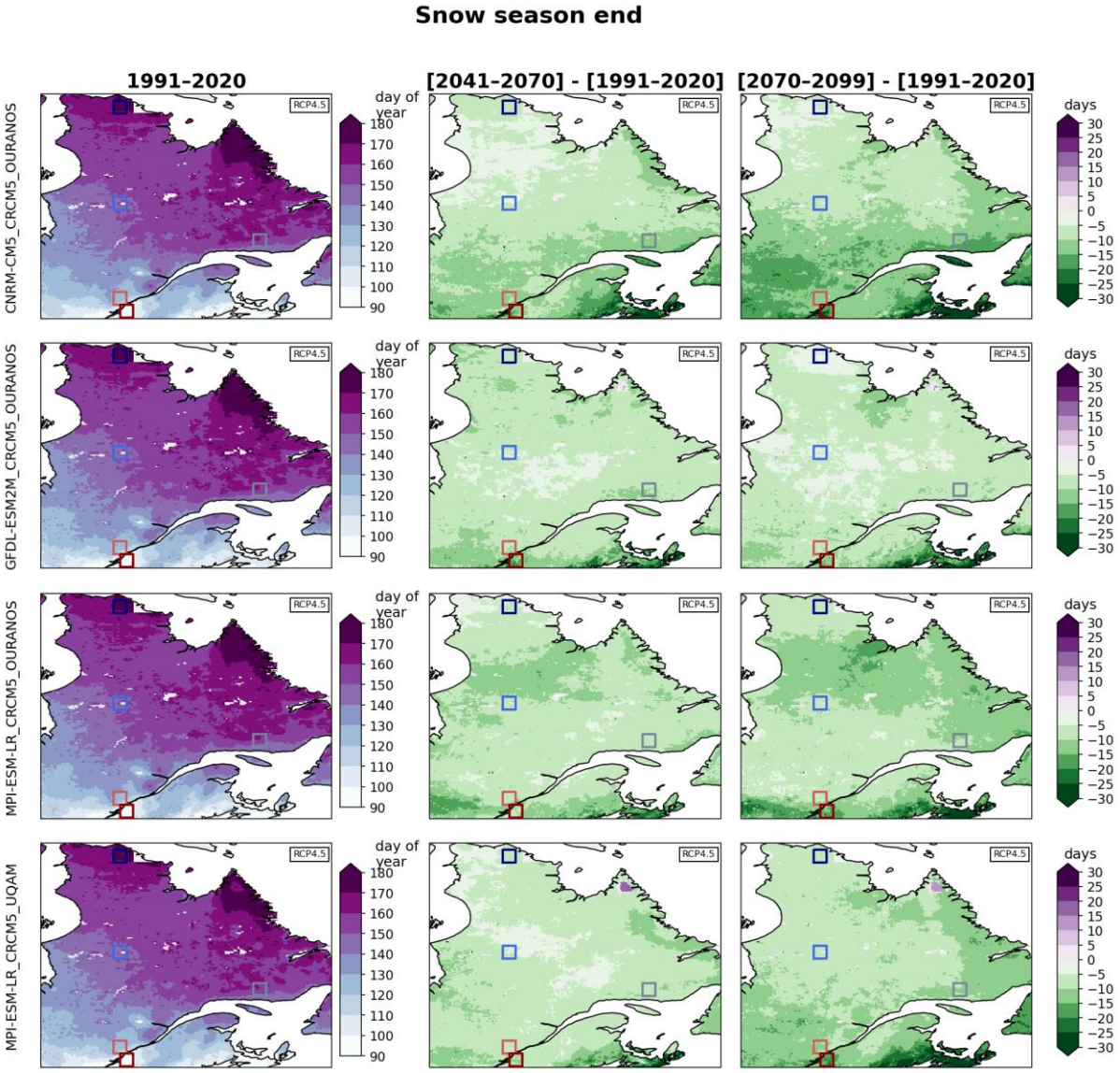

Fig. S16 Annual snow season end for 1991–2020 (left column), and differences between the 1991–2020 period and 2041–2070 (centre column) or 2070–2099 (right column). Results are presented for each simulation (row) of the RCP4.5 ensemble.

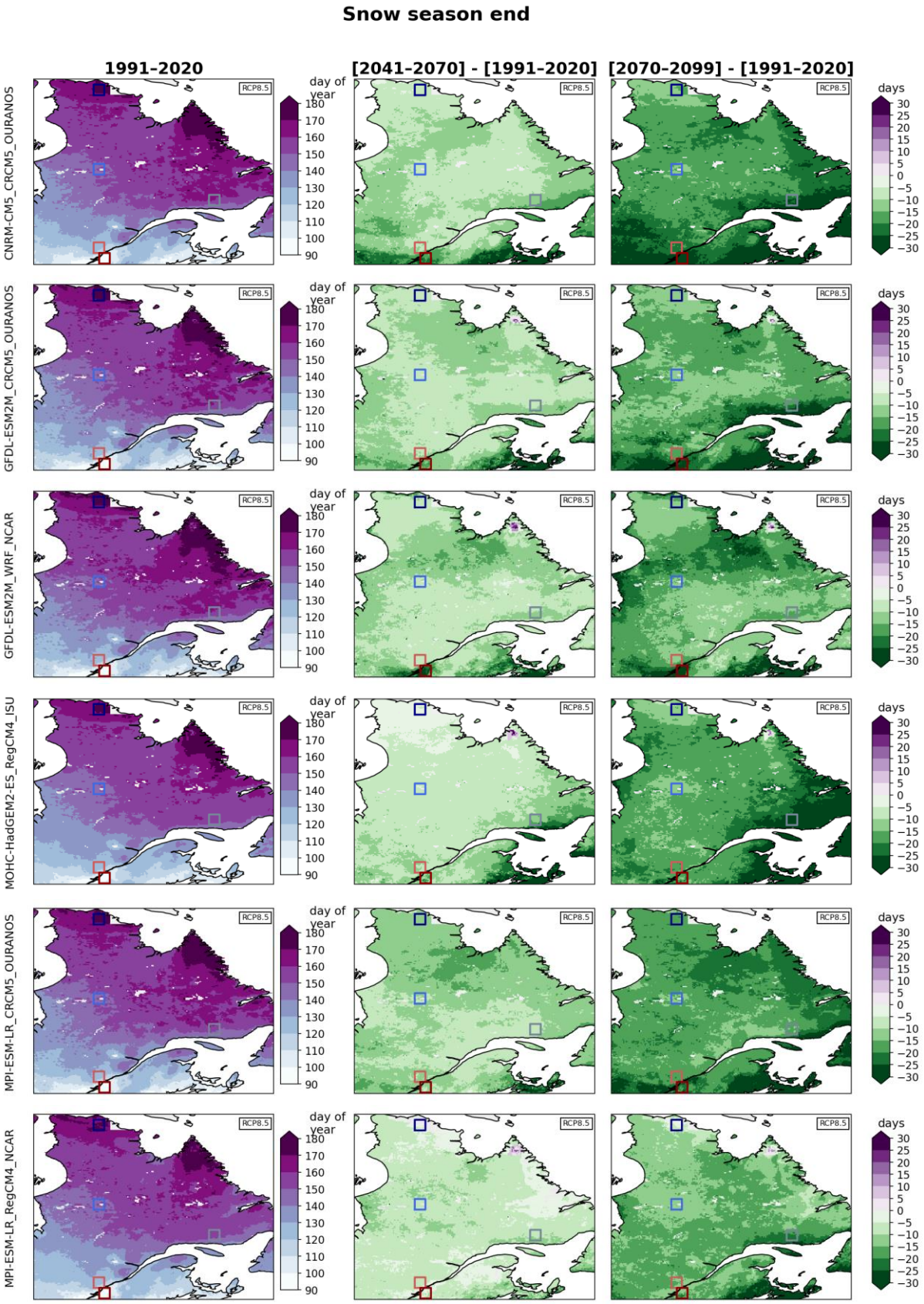

Fig. S17 Annual snow season end for 1991–2020 (left column), and differences between the 1991–2020 period and 2041–2070 (centre column) or 2070–2099 (right column). Results are presented for each simulation (row) of the RCP8.5 ensemble.

Table S1 Ensemble of simulations considered in this paper marked as X; selected simulations are marked with **X**.

		member GCM	r1i1p1	r2i1p1	r3i1p1 CanESM2	r4i1p1	r5i1p1	r3i1p1 CRCM-CM5	r1i1p1 EC-EARTH	r1i1p1 GFDL-ESM2M	r1i1p1 HadGEM2-ES	r1i1p1 MPI-ESM2M
RCM (Institution)	RCP	Resolution										
CanRCM4 (CCCma)	4.5	0.22°	X									
	8.5	0.22°	X									
CRCM5 (Ouranos)	4.5	0.22°	X					**X**		**X**		**X**
	8.5	0.22°	X	X	X	X	X	**X**		**X**		**X**
CRCM5 (UQAM)	4.5	0.44°	X									**X**
HIRHAM5 (DMI)	4.5	0.44°							X			
	8.5	0.44°							X			
RCA4 (SMHI)	4.5	0.44°	X									
	8.5	0.44°	X									
RegCM4 (ISU)	8.5	25 km								X		
RegCM4 (NCAR)	8.5	25 km									**X**	**X**
WRF (NCAR)	8.5	25 km								**X**	X	X